DEVELOPMENT OF AN ALL-COMPOSITE SPACECRAFT STRUCTURE FOR SMALL SATELLITE PROGRAMS

Timothy C. Thompson, Cathleen Grastataro, Brian G. Smith
Los Alamos National Laboratory, Los Alamos, NM

Gary Krumweide, Gary Tremblay
Composite Optics Inc., San Diego, CA

ABSTRACT

The Los Alamos National Laboratory (LANL) in partnership with Composite Optics Incorporated (COI) is advancing the development of low-cost, lightweight, composite technology for use in small satellites. The use of advanced composites in space applications is well developed, but the application of an all-composite satellite bus has never been achieved. This paper investigates the application of composite technology to the design and fabrication of an all-composite spacecraft bus for small satellites.

The satellite program Fast On-Orbit Recording of Transient Events (FORTÉ) is the second in a series of satellites to be launched into orbit for the US Department of Energy (DOE). The FORTÉ program objective is to record atmospheric bursts of electromagnetic radiation. This paper will discuss the issues of design, analysis, testing, and fabrication required to deliver the spacecraft and its associated components within a two-year period. The spacecraft will be launched into low earth orbit in late 1995 from a Pegasus-XL launch vehicle. Due to the extremely tight time constraints, a novel low-cost solution using graphite fiber reinforced plastics composites was required to achieve the performance goals of the mission. The details of material selection, characterization of design allowables, and the approach used in determining the structural geometry that will provide the optimum performance for this mission are presented.

INTRODUCTION

Overview

There is currently considerable interest in the use of low-cost, small satellites to increase the ratio of payload-to-structure performance for future missions. An inherently higher risk is acceptable for achieving long-range goals of putting many packages into orbit.

A common practice for constructing small spacecraft structures is to use an all-aluminum spacecraft bus. This reduces the payload capacity significantly, however the cost of the aluminum structure has historically been lower than one that uses advanced composites. LANL mission requirements dictate the need for a long term solution that substantially increased the ratio of payload to structural mass while maintaining a low-risk low-cost approach. LANL intends to use the concept developed for FORTÉ on future missions requiring similar enhanced payload capacities.

Mission Objectives/Science

LANL and Sandia National Laboratory are developing for space flight the FORTÉ satellite, an advanced radio frequency (RF) impulse detection and characterization experiment. Launch is scheduled aboard an Air Force Pegasus-XL vehicle in October 1995. The spacecraft will be at ±5° nadir pointing with a circular earth orbit of 800 km at a 68°-70° inclination. Mission emphasis is on the measurement of electromagnetic pulses, primarily due to lightning, within a noise environment dominated by continuous-wave carriers, such as TV and FM stations. Optical sensors such as a lightning imager and high-speed radiometer will augment the RF system in characterizing lightning events. A principal goal is to develop a comprehensive understanding of the correlation between the optical flash and the very-high-frequency emissions from lightning.

Mission science data will be made available to researchers studying lightning and the ionosphere. The extensive database generated by FORTÉ on the global distribution of lightning as detected from a satellite platform could be used in studying, for example, the correlation of global precipitation rates with lightning flash rates and locations. It is also planned to combine these data with those from simultaneous ground-based measurements as part of lightning physics campaigns.

FORTÉ will also conduct ionospheric physics experiments. The effects of large-scale structures within the ionosphere, such as traveling ionospheric disturbances and horizontal gradients in the total electron content, on the propagation of broad bandwidth signals will be studied.

Aluminum vs. Composites

LANL and its industrial partner COI are pursuing an all-graphite composite spacecraft structure. Incorporating advanced materials and unique manufacturing techniques, this structure will enable higher fractions of useful payload (as a percentage of total launch weight) to be placed in orbit. The FORTÉ experiment will provide the test bed and space validation for this structure and for other key aspects of these technologies that will be used in other space programs. This major technology development will make a significant contribution to the nation's many industrial pursuits that involve advanced spacecraft.

Staying close to known designs and well-known materials can go a long way in reducing risk and cost of the spacecraft. The original proposed design was an all-aluminum bolted structure that did not meet the weight target. Composites have a clear advantage in performance over aluminum and are required to meet the mission weight objectives.

Lab/Industry Relationship

Due to the inherent high risk, large potential payoff, and short time line, the development of such a structure for small spacecraft is appropriate for a team formed between a national laboratory and an industrial partner. The diverse skills and facilities of a national lab, teamed with an industrial collaborator having considerable experience, reduce the risk and the total cost of adding advanced technologies to the US aerospace industry's capabilities.

SPACECRAFT CONFIGURATION

Design Approach

Several factors influenced the FORTÉ design. The approach used by LANL was to do a sufficient amount of analysis to validate the design concept and to thoroughly test the concept through rigorous testing of the spacecraft. The schedule permitted two design iterations that allowed the Engineering Model (EM) to be thoroughly tested and subsequent changes to be fed back into the final flight hardware that will be constructed in the fall of 1994. The geometry is simple and modular for low cost and improved maintainability and repairability. The configuration selected allowed us to efficiently use the solar substrates as a load-bearing member. Finally, materials that are critical to the project's success have already been proven in space.

Design Considerations

The basic spacecraft configuration was dictated by the Pegasus-XL. The octagonal shape of the spacecraft lends itself to using a modular construction. Because the cost of developing and employing molded fabrication techniques is high, an approach developed at COI was adopted.

The spacecraft has several design considerations that were addressed in addition to the standard structural issues. Many payload elements have relatively tight temperature constraints because of the requirements of delicate electronic components. All payload components have to be electrically grounded. High separation shock loads require the need to mitigate shock between the bus and launch vehicle. The cage-to-deck interface requires positive metal-to-metal contact. This contact permits a well-controlled interface and efficient load transfer through the structure. In addition the spacecraft was required to have an RF shielding.

The resulting design drivers for the spacecraft bus are weight, strength, stiffness, and launch vehicle volume. The overall cost, schedule, and associated risks with performance, cost, and schedule also have a significant influence on the design.

Description of Spacecraft and Payload

The FORTÉ spacecraft primary structure consists of 6 major structural components, 3 structural trusses, 3 instrument decks, and 24 solar array substrate (SAS) panels. The fundamental principles behind this unique spacecraft design are simplicity, modularity and interchangeability, as shown in Fig. 1.

The three frame structural trusses are termed the lower, mid and upper cages. The lower and mid cages are identical to each other. Rectangular frame subassemblies comprise the lower and mid cages. The upper cage assembly is constructed using trapezoidal frame subassemblies. Eight frame subassemblies are bonded together to form each of the three octagonal cages, as shown in Fig. 2.

Fig. 1. Fully assembled spacecraft structure with SAS panels installed.

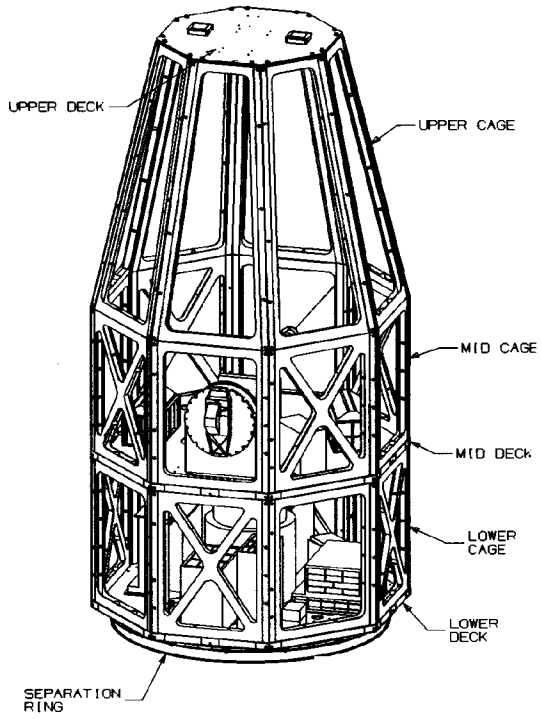

Fig. 2. Structural components of the FORTÉ spacecraft.

The three decks are termed the lower, mid and upper decks. The lower and mid decks are structurally identical to each other. Aluminum honeycomb core is sandwich-bonded between graphite/epoxy (Gr/E) skins. The upper deck closes out the structure and is fabricated from aluminum honeycomb sandwich-bonded between Gr/E skins.

The SAS panels are fabricated from the same materials as the upper deck. Aluminum inserts in the panels mate up against threaded block-type inserts in the cages. The substrates are then bolted into place.

The payload and equipment decks are the lower and mid decks respectively. The decks have aluminum threaded inserts with hole patterns and hardware sizes specifically located for each component. There are 25 different components on the three decks. Some of these components are identified in Fig. 3.

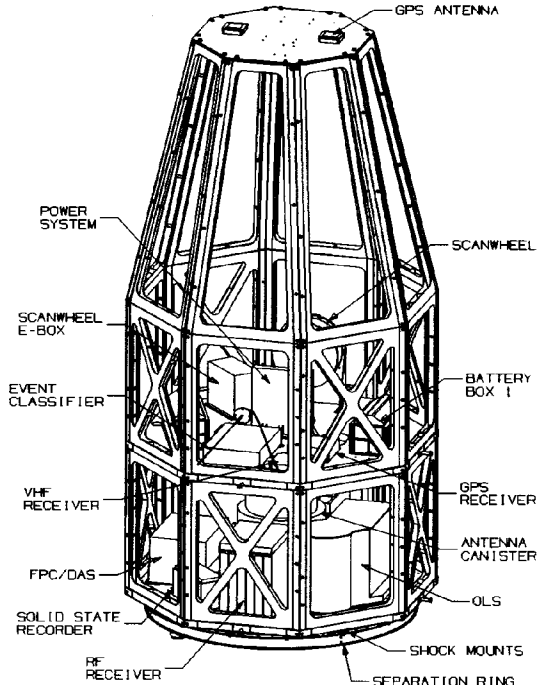

Fig. 3. Spacecraft structure with payload components.

The decks and cages are mechanically fastened to each other via aluminum corner fittings that are bonded into the cages and decks as shown in Fig. 4. This arrangement ensures that the highly loaded structure has excellent load transfer in the corners of the cage.

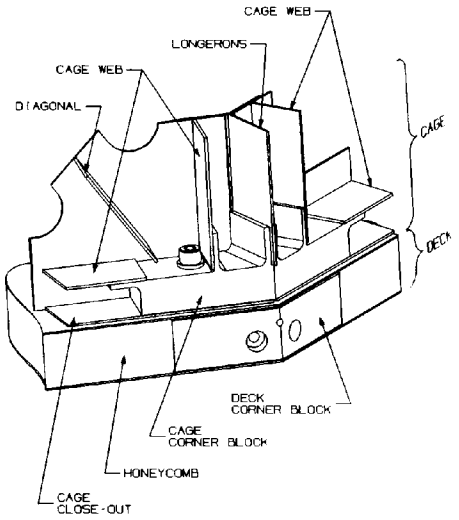

Fig. 4. Spacecraft cage structure and deck joint detail with outer skin removed for clarity.

The cross-sectional view of the cage corner is shown in Fig. 5. This view shows how the outer clip and inner clip are used to join the cage subassemblies together for a robust structural joint.

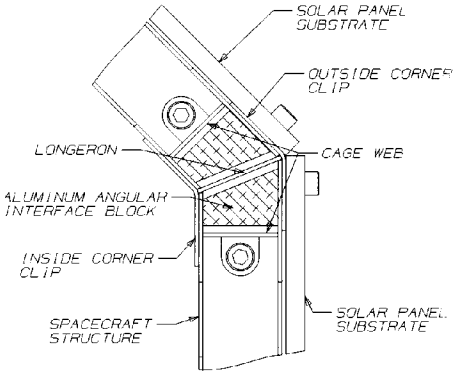

Fig. 5. Cage structure joint detail.

The shock attenuation mount and the separation ring are shown in Fig. 6. The use of a bolted joint attenuates the shock caused when the separation ring jettisons the spacecraft from the launch vehicle. The mount attenuates the shock from 3500 g to approximately 1000 g, which will protect the delicate instruments mounted directly to the lower deck.

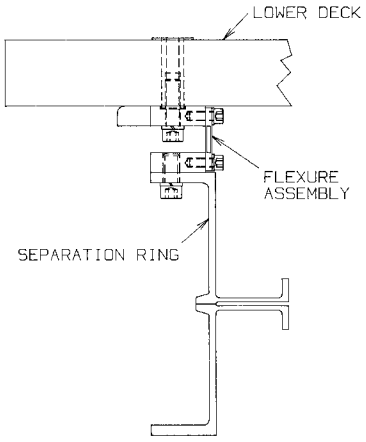

Cross-section through separation ring and flexure.

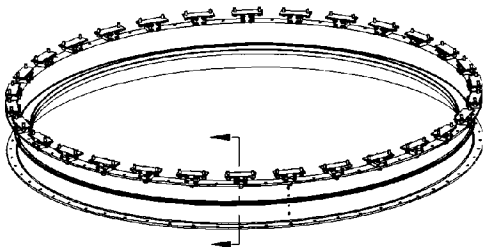

Fig. 6. Shock attenuation mount and separation ring.

STRUCTURE REQUIREMENTS

Structural Loads

The structural requirements for the FORTÉ primary spacecraft structure can be divided into two broad categories: launch phase, and on-orbit requirements. The launch phase requirements are well defined in the Air Force Small Launch Vehicle (AFSLV) interface design document, while the on-orbit specifications are set by the mission science requirements.

The launch consists of approximately 10 steps that range from dropping the vehicle from the carrier aircraft to orbit insertion and can last more than 10 minutes. Of the possible 10 steps in the launch, the initial drop from the carrier aircraft and the acceleration during the burning of the third stage create the most demands on the structure and dictate its design.

The initial drop from the carrier aircraft lasts approximately five seconds. Transient accelerations occurring at drop are dependent on the payload mass and stiffness. Because the motion is oscillatory, a large dynamic amplification occurs throughout the spacecraft. In the specific case for the FORTÉ satellite, the AFSLV design document recommended design accelerations of ±12.9 g and ±2.5 g in the lateral directions and -4.5 g in the spacecraft's longitudinal direction. After further analysis and review of the ALEXIS satellite data (not launched on Pegasus-XL), the 12.9 g acceleration was replaced with a linearly varying acceleration distribution that ranged from ±8.5 g at the bottom deck to ±18.5 g at the spacecraft upper deck, which more accurately reflected the loading conditions for the FORTÉ cantilevered spacecraft.

The other severe launch consideration is during third stage acceleration. This portion of the launch subjects the satellite to -10 g longitudinal acceleration.

Because of the need for access to payload/equipment, and to reduce weight and cost, half of the cage structure openings were left with no additional cross bracing. To do this the SAS panels must act as shear panels as well as carry the delicate solar cells. The SAS panels will react to the primary structure shear-out loads as in-plane loads. The panels were designed not only as lightweight, thermally stable panels, but also as panels capable of carrying large in-plane buckling loads and resisting extremely high shear in the vicinity of the attachment points.

On orbit the structure will be continuously temperature cycled from sun exposure to shade. Temperatures on the decks can reach extremes of -45˚C at the coldest points in the orbit to 60˚C at the warmest position, and this must be considered in the structural analysis.

DESIGN/ANALYSIS SUMMARY

The design of the FORTÉ spacecraft composite structure and solar panel substrates can best be discussed by addressing the following areas:

- mass property comparisons
- structural design heritage
- design-to-cost considerations
- parameters used in design analysis study
- dynamic loads analysis
- structural analysis summary.

Mass Property Comparisons

The original FORTÉ spacecraft was all aluminum. Switching from aluminum to graphite/epoxy produced a weight savings of approximately 46 pounds as shown in Table 1. The SAS panels (required in both designs) added an additional 33.9 pounds to both structures.

The aluminum design was from an earlier concept and did not have sufficient cross bracing, which had to be added to the later designs. An additional 30% would have to be added to the values for the three aluminum cage structures for a true weight comparison.

TABLE 1. Aluminum vs. Gr/E Weight Comparison

Component	Gr/E (lbs)	Aluminum (lbs)	Difference (lbs)
Lower Cage	17.10	16.00	-1.1
Mid Cage	17.10	16.00	-1.1
Upper Cage	19.42	25.60	6.18
Lower Deck	13.90	34.18	20.28
Mid Deck	13.80	25.69	11.89
Upper deck	2.65	3.41	.76
Shock Mounts	3.48	3.48	-
Separation Ring	8.00	8.00	-
Fasteners	-	9.60	9.60
Subtotal	95.45	141.96	46.51
Substrates	33.90	33.90	-
Total	129.35	175.86	46.51

Spacecraft mass properties are always important. The mass properties that are of interest in the FORTÉ spacecraft are mass, center of mass, and the mass moments of inertia. Table 2 shows the spacecraft mass properties for both the deployed and undeployed configurations with the bottom of the lower deck defined as Z=0. The maximum weight of the spacecraft, including all margins, is 430 lbs.

TABLE 2. Spacecraft Mass Properties

	Deployed	Undeployed
• Weight -lb	394.94	394.94
• X Bar -in	-0.13	-0.13
• Y Bar -in	0.00	0.00
• Z Bar -in	-5.86	-21.11
• IXX in^2-lbs	2.075×10^6	2.05×10^5
• IYY in^2-lbs	2.075×10^6	2.05×10^5
• IZZ in^2-lbs	9.14×10^4	8.74×10^4

Structural Design Heritage

The premise for the FORTÉ design concept originated from earlier work LANL had done for the Superconducting Super Collider (SSC) in Texas. LANL designed an ultra-stable support structure for the SSC GEM Silicon Tracker. FORTÉ is using this concept again, keeping as many of the structural components as possible similar to the original design to further reduce the cost of the structure.

Because of the apparent economic and structural benefits of this basic design approach for composite structures, engineers at LANL thought it prudent to replace the heavier aluminum design being considered for FORTÉ. LANL's subsequent structural analysis effort for FORTÉ was supported by an extensive material database that substantiated the suitability of this type of composite structural design concept.

The FORTÉ spacecraft with its fixed SAS panels has a structural design heritage from prior projects. COI developed a similar composite space frame design for the ultraviolet coronagraph spectrometer (UVCS) shown in Fig. 7. COI also developed a similar advanced composite solar panel substrate design in support of the Clementine program. The payload and equipment decks use construction techniques similar to those used for the SAS panels.

Design-to-Cost Considerations

A concept associated with composite structures is that they are much more expensive than aluminum structures. Technological advancements in the design and manufacturing of composite structures have disproved this idea. The cost of the FORTÉ spacecraft structure is very near that of the aluminum spacecraft structure it replaced. This was accomplished by using advanced design and manufacturing technology.

Fig. 7. Ultraviolet coronagraph spectrometer (UVCS).

For FORTÉ, the following design features were established to minimize manufacturing cost.

1. Design to maximize use of flat composite laminates to:
   - eliminate large production molds
   - increase the rate (pounds of prepreg per hour) at which composites can be laid up
   - minimize inspection time
   - facilitate use of programmable routers/waterjet machining
   - reduce schedule by using existing composite stock material.
2. Design in commonality between parts to:
   - minimize tooling
   - improve the learning curve (details and assembly)
   - allow laminate stacking for waterjet machining.
3. Design in self-fixturing techniques to:
   - minimize tooling
   - minimize subassembly time
   - minimize inspection time.

Along with these specific features that reduce the manufacturing cost comes a reduction in time needed to fabricate a unit. Time factors have a significant effect on the overall FORTÉ spacecraft program costs.

Parameters Used in Design Analysis Study

The basic structural parameters used in the design optimization are as follows:

- deck honeycomb thickness
- deck material thickness
- number of fasteners
- number of cross braces
- material thickness.

The skin-and-stringer FORTÉ structure utilizes the substrates to carry most of the cantilever loads in the spacecraft. This requires looking in great detail at some of the possible failure scenarios for the SAS panels and the corners of the cage structure. Table 3 shows the properties of the materials used on FORTÉ.

Dynamic Loads Analysis

The analysis effort of the FORTÉ primary structure focused on calculating the loads of the structure during the drop portion of the launch. The structure was analyzed using a general purpose finite element program, ABAQUS, to determine the maximum forces during launch. Time histories of the X-component (gravity) acceleration on the top deck, mid deck, and lower component deck are shown in Fig. 8.

TABLE 3. Material Properties

Property	Gr/E T50/ ERL1962 (in-plane)	Aluminum Honeycomb 1/8-5052-.0007	Aluminum Honeycomb 1/4-5052-.002
Elastic Modulus (psi)	10.5×10^6	7.5×10^4	1.4×10^5
Shear Modulus (psi)	3.98×10^6	4.5×10^4 L 2.2×10^4 W	6.6×10^4 L 3.0×10^4 W
Density (lbs/in^3)	0.0600	0.0018	0.0024
Poison's Ratio	0.32	.30	.30
CTE (ppm/°F)	.36	13.00	13.00
CME (ppm/%M)	218	0	0

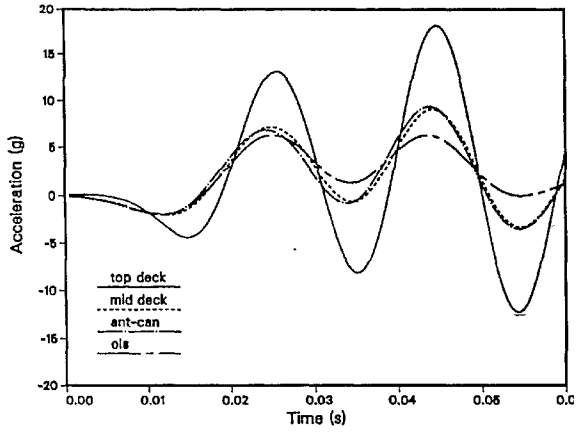

Fig. 8. Time history of the drop transient X-component acceleration.

Using the drop transient shock response spectrum for a Pegasus launch as a guide, the goal was to design the spacecraft structure so that the primary modal response would be at about 35 Hz. Preliminary analysis showed primary modes in the 20 Hz range with excessive deformation at the corners of the lower deck. Stiffeners added at the eight deck corners of the lower deck brought the primary modes up to the 50 Hz range. This is in the region of maximum response, which is not ideal, but is adequate. If the modal frequencies shift, any changes in frequency will lower these responses, which would be desirable.

A frequency analysis showed the first 19 modes to be between 35 Hz and 74 Hz. Summarized in Table 4 and illustrated in Figs. 9a through 9c are several of the key vibrational modes.

TABLE 4. Natural Modes

Mode Number	Modal Frequency (Hz)	Participating Component
1	35.7	Lower Deck
8	51.4	Body
11	53.0	Mid Deck
14	53.3	Body
16	54.3	Body

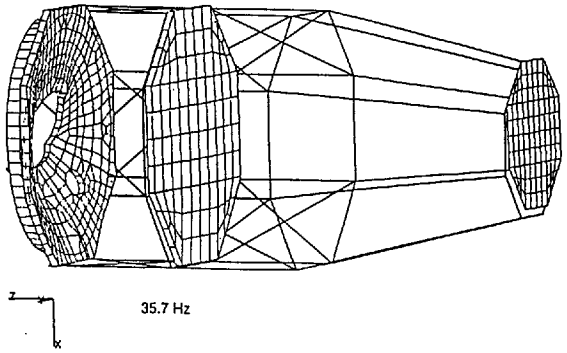

Fig. 9a. First mode lower deck.

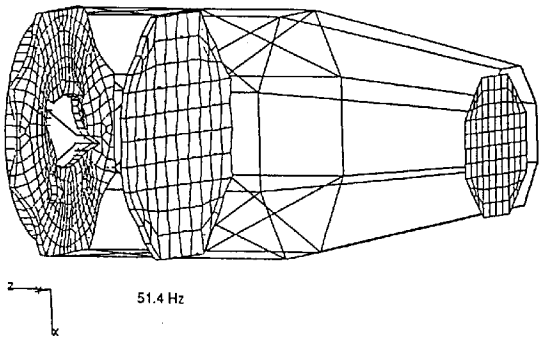

Fig. 9b. First bending body mode Y-direction.

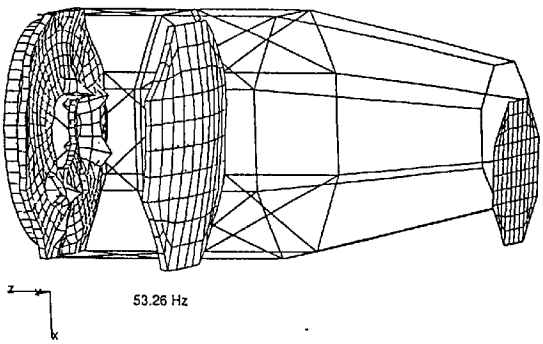

Fig. 9c. First bending body mode X-direction.

Structural Analysis Summary

The analysis effort of the FORTÉ primary spacecraft structure focused on evaluating its performance and optimizing its design for the drop portion of the launch. The structure was also analyzed during the third stage acceleration but as noted earlier this was not the critical loading condition.

A finite element model (FEM) of the structure was constructed using the COSMOS\M finite element package. The structure was modeled using three-dimensional beam elements for the longerons that would make the backbone of the structure once the cages and decks were assembled. The decks were modeled using isotropic plate elements. The mechanical properties for the aluminum honeycomb graphite skin combination were calculated and used as input. To simulate the mass of the components on the decks, the mass was distributed uniformly over the surface. The SAS panels were modeled in an identical fashion. They were attached to the rest of the structure with short beam elements so that an estimate of the in-plane shear forces could be identified. The model was fixed at its base with spring elements to simulate the shock attenuating flexures. Figure 10 shows the FORTÉ spacecraft and its associated boundary conditions.

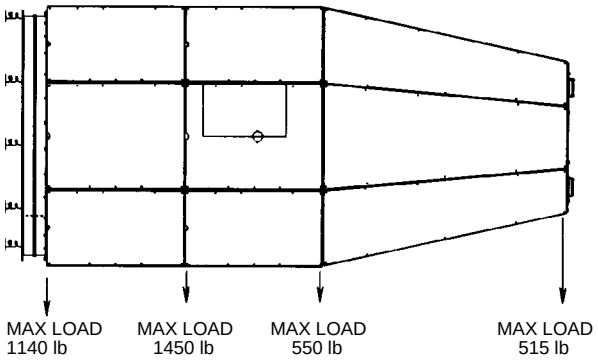

Fig. 10. FORTÉ spacecraft loading during drop.

The most severe acceleration that developed during the drop launch was a linearly varying lateral X-component acceleration of 8.5 g at the base and 18.5 g at the structure top deck. A constant lateral accelerationof 2.5 g orthogonal to the linearly varying acceleration and a longitudinal acceleration of 4.5 g compressed the structure.

The initial design had no cross bracing in the cage structure and relied solely on the solar array substrates to carry the shear from the drop transient accelerations. Analysis showed this arrangement was not feasible and studies were undertaken to determine the minimum number and location (acceptable to access requirements) of necessary cross bracing additions. In addition to the cross bracing, the number of fasteners in the substrates had to be increased from 6 per panel to 10 to meet the design allowable of 666 lbs shear-out for in-plane failure of the substrate. Figure 11 shows the component forces acting on a typical SAS panel while Table 5 shows the resultant loads.

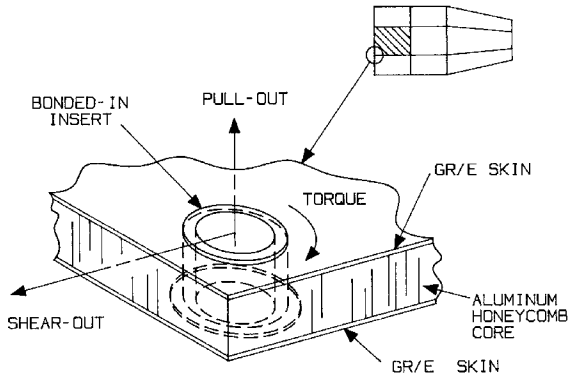

Fig. 11. SAS panel showing maximum loads.

TABLE 5. SAS Panel Resultant Loads

Load	Maximum Calculated	Allowable
Pull-Out (lbs)	5	516
Shear-Out (lbs)	265	666
Torque-Out (in-lbs)	5	72.6

Forces from the beam elements were calculated and put into a detailed model of the cage corner interface. A detailed sketch of the corner joint is shown in Fig. 12 with the results of the drop transient analysis. A detailed FEM was made of

the joint area to predict adhesive stresses. Figure 13 illustrates the joint FEM and the results are summarized in Table 6.

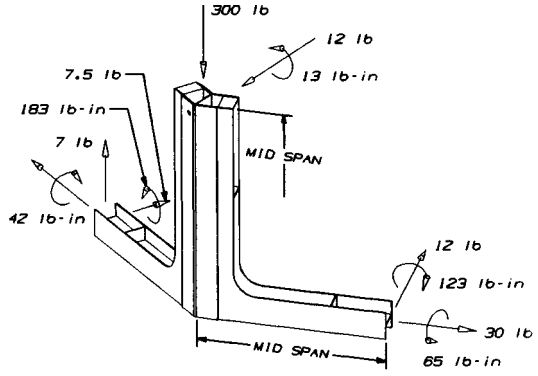

Fig. 12. Corner joint detail with maximum loading.

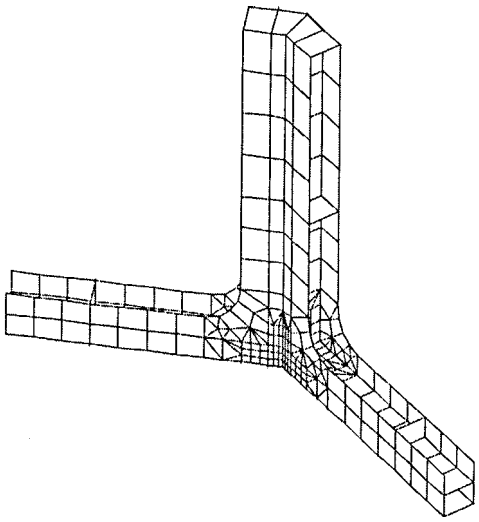

Fig. 13. FEM of the structural joint.

TABLE 6. Joint Results

Longeron-Aluminum Block Maximum in Plane Shear Stresses (psi)	324
Longeron-Aluminum Block Maximum Peel Stresses (psi)	517
Maximum Outer Skin Von Mises Stress (psi)	2500

The shear results in the SAS panels were then used to determine the buckling characteristics. The panel was analyzed using finite element and conventional composite techniques. The results are summarized in Table 7.

TABLE 7. Substrate Buckling Results

	Calculated Critical Load	Predicted Load
Column Buckling	5614 lbs	390 lbs
Face Yielding	37.7 ksi	1813 psi
Shear Crimping	2.03×10^5 psi	1.20×10^3 psi
Face Dimpling	6.67×10^5 psi	3.77×10^4 psi
Face Wrinkling	2.37×10^5 psi	3.77×10^4 psi

To gain confidence in the analytical results, modal testing was performed on the substrate panels. The first five natural frequencies were calculated using finite elements and then the panel's actual first five frequencies were found. Table 8 shows the analytical modes compared to the measured values. Figure 14 shows the experimental mode shape for a Type A panel. The natural frequencies were found by subjecting the panels to sine sweep on the function and looking for peaks on the frequency response function (FRF). The panels were excited at frequencies close to the resonance frequency and sand was used to identify the nodal points of the mode shape.

TABLE 8. Analytical and Measured Results for Fundamental Mode Shapes of a Type A SAS Panel

Mode #	FEM	FRF	% Difference
1	164.8	165	0.1%
2	203.3	214	5.0%
3	349.1	373	6.4%
4	375.5	389	3.5%

5	456.2	483	5.5%

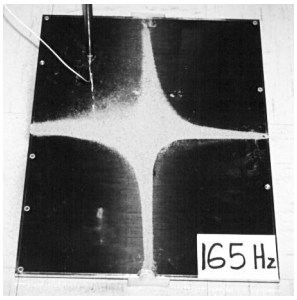

Fig. 14. Measured fundamental frequency of a Type A SAS panel.

FABRICATION

When bolted together, the 3 frame structures, 3 equipment decks, and 24 SAS panels constitute the complete primary structure for the FORTÉ spacecraft, as shown previously in Fig. 1. The following discussion addresses tooling and the various FORTÉ spacecraft structure components and illustrates the simple manufacturing approach afforded by this low-cost structure.

Tooling

The list of tooling used for the various FORTÉ structure components is very short and what could have been very complex is very simple, as depicted in Table 9.

The actual hardware (for the upper, mid, and lower decks) is used to assemble the eight frame subassemblies into upper, mid, and lower cage assemblies.

SAS Panels

The 24 SAS panels for the upper, mid, and lower cages were fabricated and machined from 8 large panels that could produce 16 lower or mid panels and 8 upper panels. The large panels were 0.020" thick precured panel assemblies of Gr/E T-50/ERL1962, [0/45/90/135] with either co-cured 0.2 mil copper on one side or co-cured 2.0 mil Kapton®. Figure 15 shows a typical cross section of an SAS panel.

These precured skins were then bonded using FM-300-2U film adhesive to .25" aluminum honeycomb core (1/8" cell; 3.1 lbs/ft^3). All aluminum inserts were post potted in Corefil 615 and bonded using room temperature epoxy adhesive, Hysol EA9394.

Insert locations were machined into the various panels at the time the sandwich subassemblies were cut from the larger panels. Then, using master bond plates that are common to those used for the corresponding frame subassemblies, all inserts were located into the SAS panel.

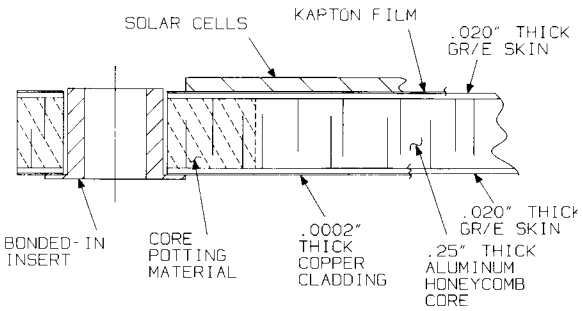

Fig. 15. Typical cross section of an SAS panel.

TABLE 9. FORTÉ Tooling List

	Component	Tool Type	Description	Qty
1	Upper, Lower & Mid decks	Bond Plate	1/4" Graphite/Tooling Resin	1
2	Lower & Mid-frames (subassys)	Bond Plate	1/4" Aluminum Plate (common to both)	1
3	Upper Frames (subassys)	Bond Plate	1/4" Aluminum Plate	1
4	Lower & Mid SAS	None required	Same 1/4" frame subassembly plate (above)	-

5	Upper SAS	None required	Same 1/4" frame subassembly plate (above)	-
6	Final assembly	None required	Self-fixturing	-

Spacecraft Structure

The space frame assemblies and equipment decks that make up the spacecraft structure differ in construction. The decks are manufactured similarly to the SAS panels, except that copper was co-cured on both sides of each deck. The space frame is made from flat laminates. The upper deck is the same thickness as the SAS panels but the mid and lower decks have a one inch thick aluminum core (1/8" cell, 4.3 lbs/ft^3). Figure 16 shows a lower deck bonded and machined. The skin thickness on all decks is 0.030" with an orientation of $[0/60/120]_S$.

The frame subassemblies are made from flat 0.048" thick laminates of T50/ERL1962 with a $[0/45/90/135]_S$ orientation. As is typical of flat laminate construction, all details can be "nested" tightly on larger cured laminates and machined out with a waterjet machining head mounted to a programmable router. Figure 17 shows all the details for FORTÉ structure nested on two laminates. Four laminates of one configuration and two laminates of the other configuration were machined.

Utilizing COI's concept for a self-fixturing fabrication process (the Short Notice Accelerated Production Satellite or SNAPSAT$^{TM*)}$, all details are removed from a completely processed panel (prepped for bonding) and "snapped" together. The snapping together feature uses mortise and tenon joints that are precision machined into the details. Figure 18 shows the tool setup for bonding ribs to an upper frame skin (the second skin has yet to be bonded).

Note that the frame subassemblies (two skins and ribs bonded together) have only bonded in at this subassembly stage those metal fittings to which the SAS panels attach. Figure 19 shows a portion of this frame assembly. Note that blade longerons and inner and outer angle clips are not bonded at this time. The deck angular interface fittings are what initially ties the structure together. These are visible in Fig. 20. Figure 21 shows the corner splicing angles installed that cover up the blade longeron, and illustrates how the upper and lower decks are used to assemble the frame. Also shown are the angular interface fittings ready to accept the mid frame subassemblies. Note the copper plating on this lower frame assembly. This electroplated copper was plated on the outer surface of outside panels only. Figure 22 shows the SAS panels being fitted to the lower frame assembly. Because of common tooling, the fit was exact. All SAS panels are interchangeable.

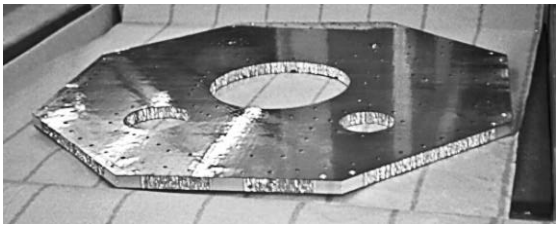

Fig. 16. Lower deck.

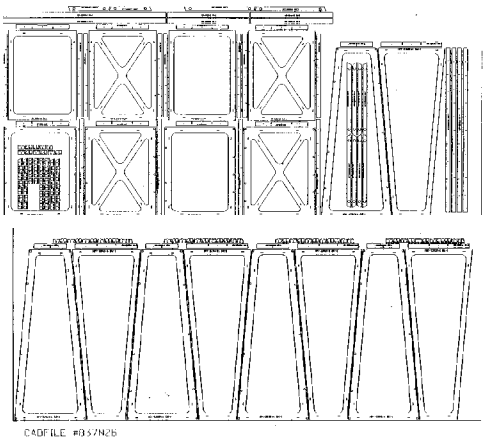

Fig. 17. Water jet cutting pattern showing the nesting of components using flat stock Gr/E.

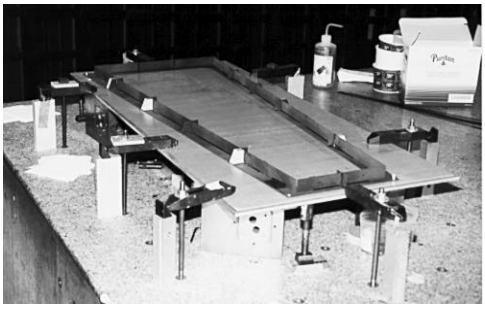

Fig. 18. Structural bonding of ribs.

* SNAPSAT^{TM} is a patent-pending trademark of COI.

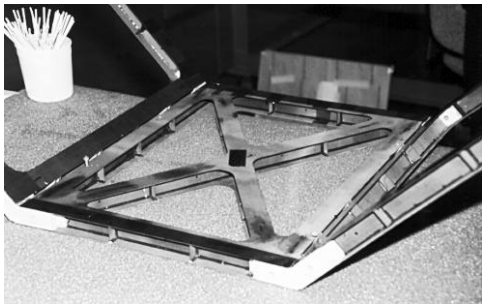

Fig. 19. Cage panel frame subassembly showing the interface fittings.

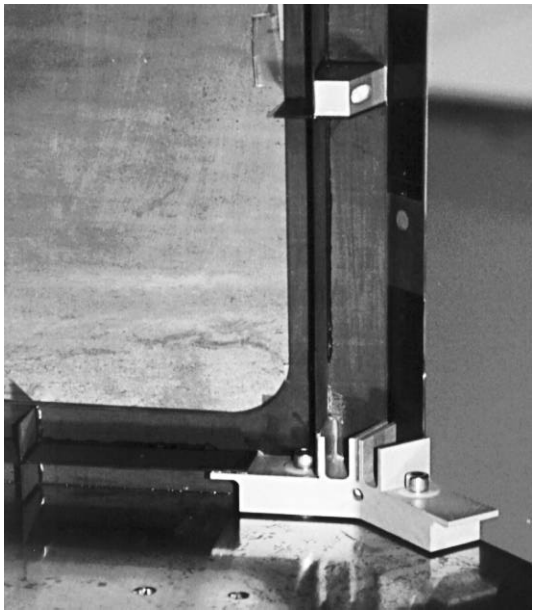

Fig. 20. Cage corner detail.

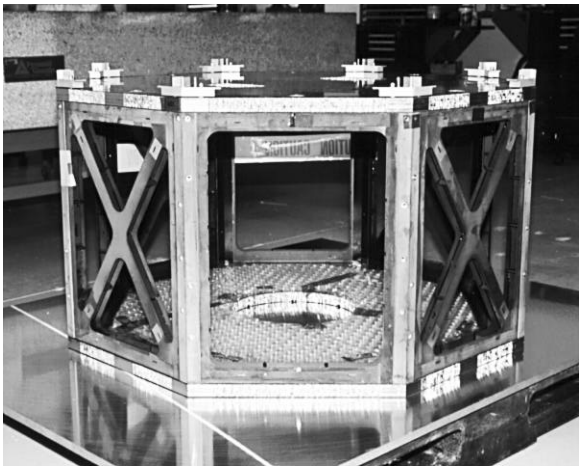

Fig. 21. Structural splicing angles.

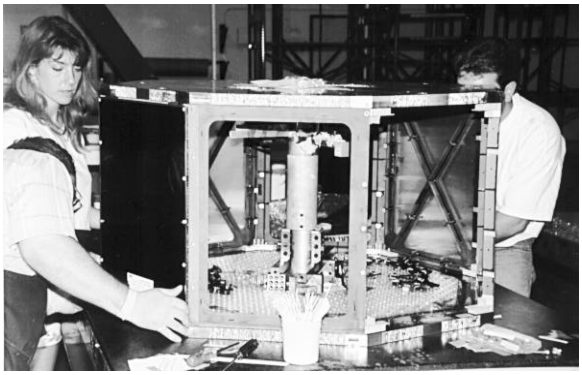

Fig. 22. SAS panels being fit to the lower frame assembly.

Final Assembly

By repeating the above process for all decks and frames, the final assembly shown in Fig. 23 is achieved. The SAS panels have not yet been installed. Note that the mid and upper frame assemblies are unplated for this first unit. This was done in order to evaluate the RF shielding effectiveness of unplated vs. plated Gr/E. Pending the electromagnetic interference (EMI) test results on the EM, the flight unit will be configured for EMI protection. The copper on the back of the SAS panels provides the EMI protection for the spacecraft equipment and also serves to electrically shield the spacecraft from its antenna system.

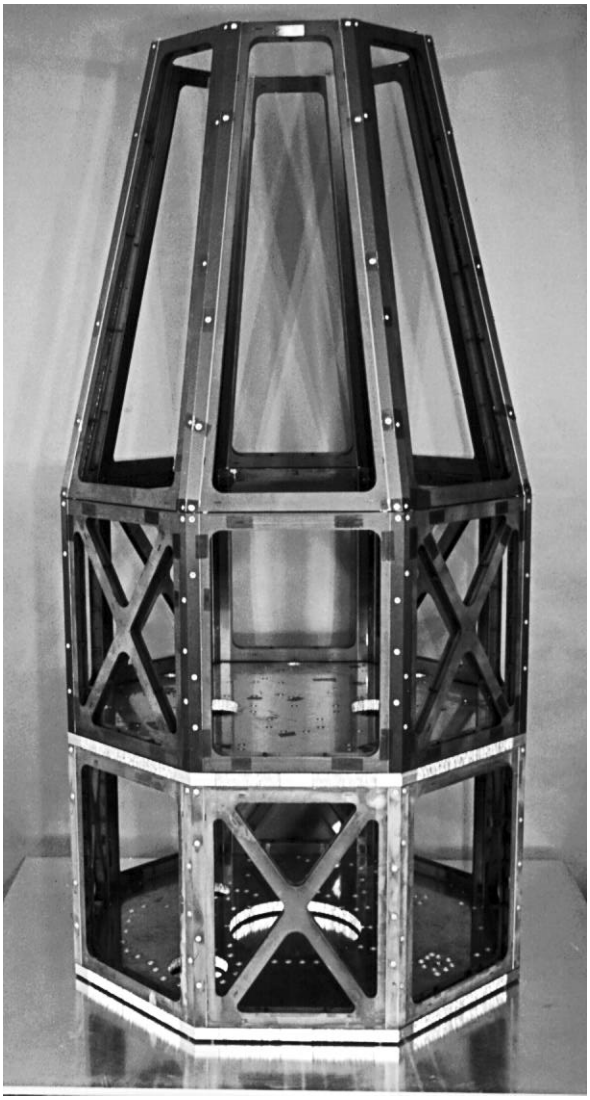

Fig. 23. Final spacecraft assembly.

TESTING

Material Testing

The uniqueness of the FORTÉ primary spacecraft structure meant that some of the detailed design information was lacking. Parts of other spacecraft devices were similar but not exactly the same. A testing effort was initiated to define design allowables in critical areas. The primary concerns were the high shear stress areas of the SAS panels, the shear stress between the graphite and the aluminum angular interface block corner joints, and the deck component insert pullout allowables.

The SAS panels were viewed as the most critical area of the structure and no design data existed for them. Edge coupons were fabricated by COI and tested at LANL. The coupons were designed to carry a maximum shear load through the corner of the coupon since analysis showed the maximum shear force was along this direction. Along with determining the absolute design allowables there was also an interest to know the effects of thermal cycling on the bonded joints.

The spacecraft would be maintained near room temperature during the launch phase, but it would be cycled from -65°C to 80°C five times prior to launch as part of its qualification testing. Therefore it would be imperative to know the effects of thermal cycling on the shear-out design allowable. Ten coupons were tested with thermal cycling and ten coupons were tested without thermal cycling. The cycle commenced at room temperature with the cooling to -65°C at a rate of 10°C/min. This extreme was held for 10 minutes and then the part was heated to 80°C at 10°C/min and held at that extreme for 10 minutes. Then the part was returned to room temperature. This cycle was repeated five times. All coupons were then tested at room temperature.

The results of the two tests are summarized in Table 10. The average ultimate shear-out load for the thermal cycled coupons degraded by 13% and the design allowable was decreased by 24%.

Ten additional coupons were tested after a modified thermal cycle. The extreme temperatures were held for one hour. The increased soak times at the extreme temperatures only decreased the mean ultimate shear-out load an additional 9% and the design allowable an additional 17%.

TABLE 10. Corner Static Load Test

	Mean Ultimate Shear-Out (lbs)	Allowable Shear-Out (lbs)
All Coupons Combined	940	750
Non Thermal Cycled Coupons	1003	881
Thermal Cycled Coupons	877	666

Another critical area for which little design data existed is the cage structure corners where aluminum angular interface blocks are bonded to the graphite skins. Initially the published shear strength for the adhesive was used to determine the design allowable. Fifteen single lap shear coupons were fabricated and tested at COI. Of the 15, 5 were not thermally cycled and 10 were subjected to the same thermal cycle as the corner coupons. The mean ultimate shear load showed no dependence on thermal cycling. The design allowables varied substantially, ranging from 507 psi for all 15, 473 psi for only the thermally cycled set, to 231 psi the non-thermal-cycled set. The very low value for the non-thermal-cycled set is a reflection of the small sample set size, given that the mean and standard deviation are almost identical to those of the other cases (Table 11).

TABLE 11. Shear Coupon Load Test

	Measured Bulk Area Mean Ultimate Shear Stress (psi)	Calculated Bulk Area Allowable Shear Stress (psi)
All Coupons Combined (15 Coupons)	895	507
Non-Thermal-Cycled (5 Coupons)	888	231
Thermal-Cycled (10 Coupons)	900	438

Analytical solutions and FEMs of the coupons were created to determine the stress distribution at failure. The analytical solution suggested by Ojalvo and Eidinoff (1977) shows a bulk shear stress of approximately 660 psi and a peak at the edge of the bond area of more than 5000 psi. Their results indicate a peak peel stress at the bond edge of 3550 psi. A plane two-dimensional model showed the same stress distributions as suggested by the analytical solutions but a bulk area shear stress of about 125 psi and a corresponding peak of 8600 psi (Fig. 24: the stresses are plotted from the bonded joint center to the edge because of symmetry). Figure 25 shows the peel stress vs. bonded joint length (also plotted from the joint center). The bulk area peel stress is initially close to zero, then becomes compressive near the edge and peaks at the very edge at almost 13,500 psi.

The actual joint in the FORTÉ structure unfortunately does not resemble the lap shear coupons. In the structure a relatively thin graphite skin is bonded to a relatively massive aluminum block (Fig. 4). Therefore, further study of the lap shear finite element model was done to determine the effect of considerably increasing the thickness of one adherent on the stress distribution. The results showed a dramatic change in both the shear and peel stresses. The bulk area shear stress was reduced slightly to 580 psi (Fig. 26). The shear stress then peaks at the bond edge at slightly over 3800 psi. The bulk area peel stress, as shown in Fig. 27, is initially 170 psi and increases to 435 psi. The peel stress then peaks at the bond edge at -2227 psi. These results indicate that the peel stress is reduced significantly when one adherent is much thicker than the adhesive and the other adherent.

The results also show that the bulk area shear stresses are lower than those determined from the lap shear coupons tests (indicated in Table 11). To determine those values the ultimate load was divided by the bond area. From the finite element model shown in Fig. 13 the maximum shear stress calculated was 324 psi and the peak peel stress was 517 psi, far below the analytical results or the finite element predictions. These are slightly larger than the allowables determined by testing, but when compared to the analytical results or the FEMs the peak stresses may be considered acceptable.

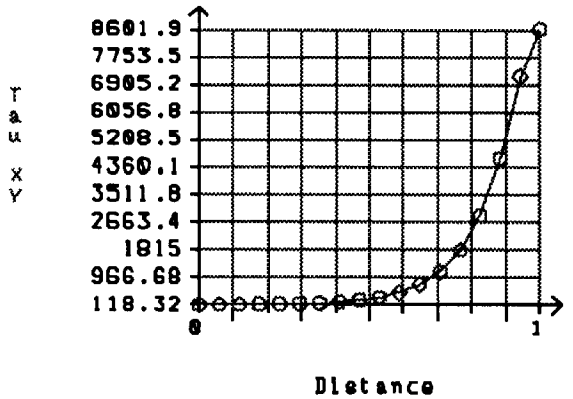

Fig. 24. Adhesive midplane shear stress.

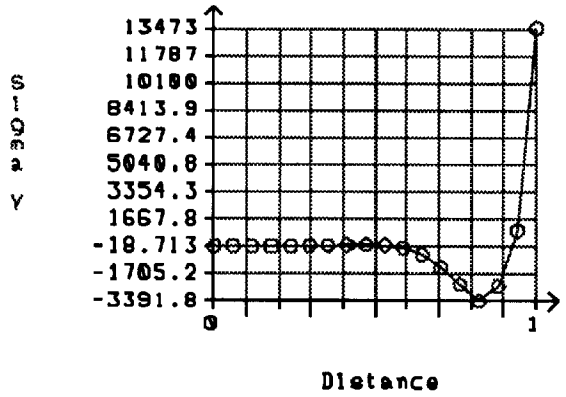

Fig. 25. Adhesive top-plane peel stress.

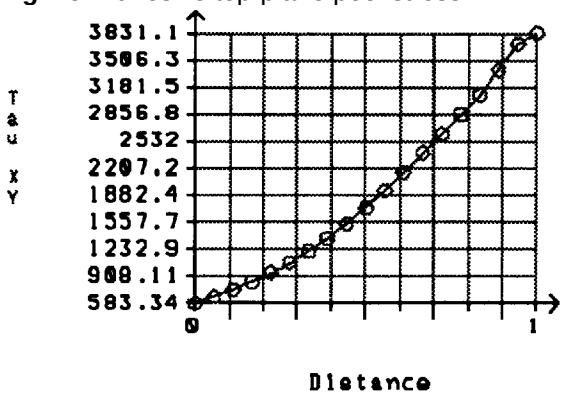

Fig. 26. Adhesive midplane shear stress.

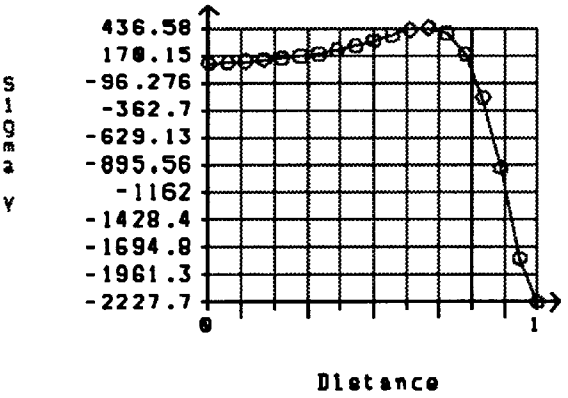

Fig. 27. Adhesive midplane peel stress.

The last area where testing was required to provide accurate design data was for the deck inserts. A deck coupon with twelve inserts was made and tested by COI. The results of this test are shown in Table 12. The deck inserts are not bonded in place but rather are held secure by a threaded fastener as shown in Fig. 28. Therefore, thermal cycling is not an issue with these inserts.

TABLE 12. Deck Inserts Pull-Out Results

	Mean Ultimate Load (lbs)	Allowable Load (lbs)	Maximum Calculated Load at Launch (lbs)
Pull-out	659	493	143
Shear-out	877	660	158

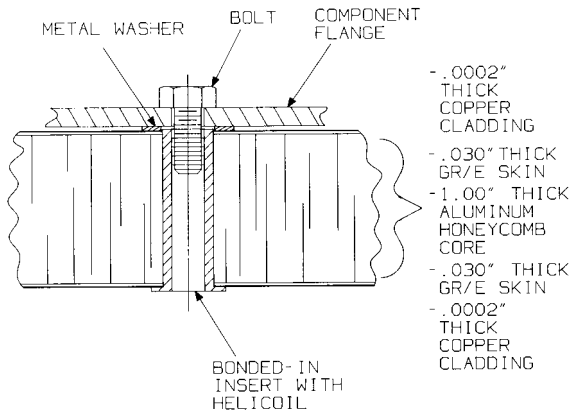

Fig. 28. Deck fastener detail.

Acceptance testing of the assembled engineering model structure will be performed at COI. Three types of tests are planned: a thermal cycling test, lateral static load tests, and a longitudinal static load test. Before commencing any acceptance testing, and after each test, the structure will be thoroughly inspected by the coin-tap method. If problems are detected from a coin-tap examination that cannot be resolved, then more extensive methods will be employed, such as ultrasound or thermography.

The entire structure will be subjected to the identical thermal cycle that the corner coupon was run through for its shear-out tests. The structure will be cooled from room temperature to -65°C at 10°C/min and held at -65°C for 15 minutes. It will then be warmed to 80°C at 10°C/min and held at 80°C for 15 minutes. The cycle will be repeated five times. The main purpose of the cycle is to submit the structure and eventually the assembled flight article to identical circumstances as the components . The temperature of the structure will be monitored during thermal cycling.

After thermal cycling the structure will be submitted to lateral static load testing. The

structure will be mounted to the floor and forces that simulate the design drop transient accelerations will be applied (see Fig. 10). The corresponding loads are 1140 lbs at the bottom deck, 1450 lbs at the mid deck, 550 lbs at the transition area, and 515 lbs at the top deck. During loading, deflections will be monitored at each point of load application and in the same plane but in the orthogonal direction. The structure will then be rotated 90 degrees about the longitudinal axis and the procedure repeated three additional times.

Strain gauges will be mounted to both sides of the SAS panels located over the cage structure with cross members. One of the corner joints will also be equipped with strain gauges to monitor loads going into perceived critical areas of the structure.

The structure decks will then be loaded to simulate a -10 g longitudinal acceleration on the structure. The corresponding loads are 1590 lbs on the bottom deck, 1600 lbs on the mid deck, and 860 lbs on the top deck. The same strain gauges will be monitored.

CONCLUSIONS

LANL and COI have designed, analyzed, and demonstrated a simplified, cost-effective method for the production of small satellite spacecraft structures. This process produces an all-composite spacecraft structure that is lightweight and very strong, providing substantial improvement over aluminum designs in its payload-to-weight ratio. The fabrication technology that has been developed produces savings in production time and expense over previous composite processes. It is competitive with aluminum structure processes in expense and speed of production and is applicable to a wide variety of structures. The simple but robust spacecraft structure provides a platform that will be useful for a wide variety of applications.

ACKNOWLEDGMENTS

This work is supported by the US Department of Energy.

The lightning imager utilizes the design developed by Dr. Hugh Christian, NASA/MSFC.

We gratefully acknowledge Tom Butler, Peggy Goldman, Manuel Gomez, Rick Hinckley, Dr. Stephen Knox, Charles Johnson, Roger Smith and Erik Swensen for their contributions to this paper.

REFERENCES

Goland, M. and E. Reissner, “The Stresses in Cemented Joints,” Journal of Applied Mechanics, March 1994, Vol. 11, pp. A17-A27.

Griiffin, M. D. and J. R. French, *Space Vehicle Design*, AIAA Publishing, 1991, pp. 345, 351, 356.

“Mechanical Properties of Hexcel Honeycomb Materials,” Hexcel TSB 120, Hexcel Corporation, 1987.

“Guidlines for the Presentation of Data,” MIL-HDBK-5D, June 1, 1983.

Kilpatrick, M., J. Girard, K. Dodson, “Design of a Precise and Stable Telescope Structure for the Ultraviolet Coronagraph Spectrometer (UVCS),” SPIE, Volume 1690, Design of Optical Instruments, 1962.

Ojalvo, I. U., and H. L. Eidinoff, "Bond Thickness Effects Upon Stresses in Single-Lap Adhesive Joints,” AIAA Journal, Vol.16, No.3, 1977.

Pegasus Air Force Small Launch Vehicle Interface Design Document, Release 1.00, August 31, 1993.

“The Basics on Bonded Sandwich Construction,” Hexcel TSB 124, Hexcel Corporation, 1984.